

[22] Modeling action of a hyperspectrometer based on the Offner scheme within geometric optics

Kazanskiy N.L., Kharitonov S.I., Karsakov A.V., Khonina S.N.
Image Processing Systems Institute, Russian Academy of Sciences
Samara State Aerospace University

Abstract

We considered comparative modeling action of a hyperspectrometer based on the Offner scheme including prisms or a diffraction grating within the geometrical optics. It is shown that the use of a diffraction grating instead of a prism results in a more uniform spread of the spectral components of the dispersed image. Key-words: hyperspectrometer, Offner scheme, dispersive element, spectral image components.

Citation: KAZANSKIY N.L. GEOMETRICAL-OPTICAL MODELING OF AN OFFNER HYPERSPECTROMETER / KAZANSKIY N.L., KHARITONOV S.I., KARSAKOV A.V., KHONINA S.N. // COMPUTER OPTICS. – 2014. – VOL. 38(2). – P. 271-280.

Introduction

It is possible to attain a considerably higher efficiency in the use of earth remote sensing (ERS) data by conducting a detailed analysis of the data at different wavelengths [1 – 3]. To these ends, compact imaging hyperspectrometers with high spatial and spectral resolution have been designed. Prior to the advent of the imaging spectrometers, the reflection and radiation spectra of the Earth surface were rarely used as identification markers [1 – 4], although they had been well known and studied for decades. Poor geometric resolution of the airborne spectrometers, their ability to provide data only along a flight path and from extended ground objects made such spectra poorly suited for the purpose. The advent of imaging spectrometers has become possible due to advances in technology: development of matrix receivers and polychromators with high spectral resolution. Imaging spectrometers are made up of two systems: (1) an optical system that breaks down the spatial region under analysis into a set of adjacent points and (2) an imaging spectrometer that decomposes the registered electromagnetic radiation into separate spectral bandwidths. Thus, an imaging spectrometer forms a multi-dimensional spatial-spectral image with every image pixel having its own spectrum. Such an image is called a data cube, with two dimensions containing the terrain image on a surface and the third dimension containing the image spectral properties. State-

of-the-art imaging spectrometers have a spectral resolution of 1.8 – 2.0 nm, sensing spectral characteristics of the underlying terrain found in the instruments' instantaneous viewing field (1 mrad in airborne spectrometers).

For particular purposes, different types of imaging hyperspectrometers are utilized, including dispersion, filtering and interference hyperspectrometers. Various schemes of hyperspectrometers used for earth remote sensing can be found in Ref. [5–31]. The majority of tasks can be solved using a conventional dispersion hyperspectrometer. A detailed description of a compact imaging spectrometer (COMIS) mounted on board a Korean microsatellite STSAT3 can be found in Ref. [7–10]. The microsatellite of size 85x82x100-cm has a weight of 150 kg. Alongside the spectrometer, the satellite carries a multi-purpose infrared imaging system (MIRIS) intended to sense the Galaxy in the IR range.

The dispersive component of the spectrometer may be in the form of both a prism and a diffraction grating. An obvious advantage of the diffraction grating over the prism is its compactness. The imaging spectrometers that employ the diffraction grating as a dispersive component are usually based on the Offner or Dyson scheme [7–31].

In this work, we model the performance of an Offner hyperspectrometer using a geometrical optics approach, comparing the dispersive characteristics of prism-based and grating-based schemes.

1. Mathematical tools to simulate the performance of a hyperspectrometer in the geometrical optics

For a hyperspectral datacube [2, 3] to be generated, images obtained by means of hyperspectral facilities need to undergo processing and filtering procedures. This requires the knowledge of a variety of instrument functions, such as the point spread function. When using the hyperspectral equipment, an image pixel turns into a line, with each pixel of the latter containing spectrum-related data.

To be able to calculate the intensity distribution in the focal region it is required to trace the rays in the optical system. The hyperspectrometer is made up of a telescopic component and a hyperspectral unit (Fig. 1).

The scheme of an Offner spectrometer is composed of three mirrors, an input slit, and an image plane (Fig. 1). The input slit is located in a plane perpendicular to the z-axis, passing through curvature centers of all three mirrors. The first and third mirrors have radius R, the second mirror has radius R/2. In some schemes, the first and third mirrors are designed as a single mirror (Fig. 1). An outgoing ray from the source incident on the first mirror experiences reflection and falls onto a grating located on the second convex spherical mirror. Then, the ray is reflected from the third mirror before coming to the registration plane. Design techniques for the telescopic component have been described elsewhere, e.g. see [32]. The aim of this work is to perform geometric-optical modeling of the hyperspectral unit.

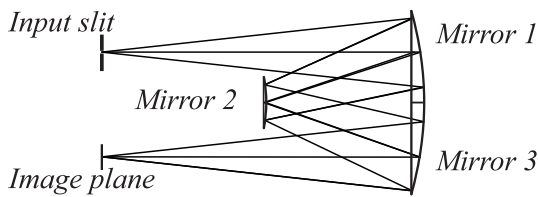


Fig. 1. Ray tracing in an optical setup.

Intersection of the ray with the first mirror

Let there be a ray reflected from a spherical surface $x^2 + y^2 + z^2 - R^2 = 0$. (1)

The ray is assumed to outgo from point x_0, y_0, z_0 , arriving at point u_1, v_1, Z found at the surface of the first sphere. The unit vector is given by

$$\vec{s}_0 = \frac{\vec{S}_0}{S_0} = \frac{(u_1 - x_0)\vec{i} + (v_1 - y_0)\vec{j} + Z(u_1, v_1)\vec{k}}{\sqrt{(u_1 - x_0)^2 + (v_1 - y_0)^2 + Z^2(u_1, v_1)}} = \frac{\vec{r}_1 - \vec{r}_0}{|\vec{r}_0 - \vec{r}_1|}, \quad (2)$$

$$\vec{r}_0(u_1, v_1) = u_1\vec{i} + v_1\vec{j} \quad (3)$$

$$\vec{r}_1(u_1, v_1) = \vec{N}(u_1, v_1) = u_1\vec{i} + v_1\vec{j} - Z_1(u_1, v_1)\vec{k}$$

$$S_0(u_1, v_1) = \sqrt{(u_1 - x_0)^2 + (v_1 - y_0)^2 + Z^2(u_1, v_1)}. \quad (4)$$

The normal vector is

$$\vec{N}(u_1, v_1) = \vec{r}_1(u_1, v_1) = u_1\vec{i} + v_1\vec{j} - Z_1(u_1, v_1)\vec{k}. \quad (5)$$

The normalized vector is

$$\vec{n}_1(u_1, v_1) = \frac{\vec{N}(u_1, v_1)}{N(u_1, v_1)}, \quad (6)$$

$$r_1(u_1, v_1) = N(u_1, v_1) = \sqrt{u_1^2 + v_1^2 + Z^2(u_1, v_1)}. \quad (7)$$

The reflection law in the vector form reads as

$$[\vec{n}_1 \times \vec{s}_0] = [\vec{n}_1 \times \vec{s}_1], \quad (8)$$

$$\vec{n}_1 \times [\vec{n}_1 \times \vec{s}_0] = \vec{n}_1 \times [\vec{n}_1 \times \vec{s}_1], \quad (9)$$

$$\vec{n}(\vec{n}, \vec{s}_0) - \vec{s}_0 = \vec{n}(\vec{n}, \vec{s}_1) - \vec{s}_1. \quad (10)$$

The unit vector of the reflected ray takes the form:

$$\vec{s}_1(u, v) = \vec{s}_0(u_1, v_1) - 2\vec{n}_1(u_1, v_1)(\vec{n}_1(u_1, v_1), \vec{s}_0(u_1, v_1)). \quad (11)$$

Substituting the relations for the unit vector of the incident ray and the normal vector yields:

$$\vec{s}_1(u_1, v_1) = \frac{\vec{r}_0 - \vec{r}_1}{|\vec{r}_0 - \vec{r}_1|} - 2 \frac{\vec{r}_1}{r_1} \left(\frac{\vec{r}_1}{r_1}, \frac{\vec{r}_0 - \vec{r}_1}{|\vec{r}_0 - \vec{r}_1|} \right). \quad (12)$$

In this case, the ray transform takes the form:

$$\vec{r}(u_1, v_1, l) = \vec{r}_1(u_1, v_1) + \vec{s}_1(u_1, v_1)l. \quad (13)$$

Intersection of the ray with the second sphere

Following the reflection at the first sphere, the ray intersects the second sphere, experiencing reflection.

The equation of the second sphere is

$$F_2(\vec{r}) = 0. \quad (14)$$

For a sphere of radius R / 2, the equation takes the form:

$$F_2(\vec{r}) = (\vec{r}, \vec{r}) - \frac{R^2}{4} = 0. \quad (15)$$

The intersection point with the ray is derived from the condition

$$F_2(\vec{r}(u_1, v_1, l)) = 0, \quad (16)$$

$$(\vec{r}_1(u_1, v_1) + \vec{s}_1(u_1, v_1)l)^2 - \frac{R^2}{4} = 0. \quad (17)$$

This equation can be reduced to a quadratic form

$$l^2 + 2(\vec{r}_1(u_1, v_1), \vec{s}_1(u_1, v_1))l_1 + r_1^2(u_1, v_1) - \frac{R^2}{4} = 0. \quad (18)$$

Solving Eq. (18) for l_1 , the intersection point with the second sphere is given by

$$\vec{r}_2 = \vec{r}_1(u_1, v_1) + \vec{s}_1(u_1, v_1)l_1. \quad (19)$$

The intersection point with the second sphere is given by the coordinates (u_2, v_2) :

$$(u_2, v_2) = \vec{r}_{2\perp} = \vec{r}_{1\perp}(u_1, v_1) + \vec{s}_{1\perp}(u_1, v_1)l_1.$$

The unit vector of the ray reflected from the second sphere is

$$\begin{aligned} \vec{s}_2(u_2, v_2) &= \vec{s}_1(u_1, v_1) - \\ &- 2\vec{n}_2(u_2, v_2) \left(\vec{n}_2(u_2, v_2), \vec{s}_1(u_1, v_1) \right), \end{aligned} \quad (20)$$

$\vec{n}_2(u_2, v_2)$ is the normal to the second surface drawn at the intersection point (u_2, v_2) after reflection from the first surface. With a diffraction grating located on the second sphere, there are several reflected rays. The diffraction grating is a particular case of a diffractive optical element (DOE) on a curvilinear surface. In Section 2, the general theory of diffraction of light by a DOE located on a curvilinear surface is set forth.

Intersection of the ray with the third sphere

Following reflection from the second sphere, the ray intersects the third sphere, experiencing reflection. The ray reflected from the second sphere is given by

$$\vec{r}_2 = \vec{r}_1(u_1, v_1) + \vec{s}_1(u_1, v_1)l_1 + \vec{s}_2(u_2, v_2)l_2. \quad (21)$$

The intersection with the third sphere of radius R is described by the equation:

$$\left(\vec{r}_1(u_1, v_1) + \vec{s}_1(u_1, v_1)l_1 + \vec{s}_2(u_2, v_2)l_2 \right)^2 - R^2 = 0. \quad (22)$$

Solving Eq. (22) for l_2 , we get the intersection point with the third sphere of radius R . The coordinates (u_3, v_3) of the intersection point with the third sphere are derived from the relation:

$$\begin{aligned} (u_3, v_3) &= \vec{r}_{3\perp} = \vec{r}_{1\perp}(u_1, v_1) + \\ &+ \vec{s}_{1\perp}(u_1, v_1)l_1 + \vec{s}_{2\perp}(u_2, v_2)l_2. \end{aligned} \quad (23)$$

The unit vector of the ray reflected from the third sphere is

$$\begin{aligned} \vec{s}_3(u_3, v_3) &= \vec{s}_2(u_2, v_2) - \\ &- 2\vec{n}_3(u_3, v_3) \left(\vec{n}_3(u_3, v_3), \vec{s}_2(u_2, v_2) \right), \end{aligned} \quad (24)$$

$\vec{n}_3(u_3, v_3)$ is the normal to the third sphere of radius R drawn at the point of intersection of the ray reflected from the second surface at point (u_3, v_3) .

Ray intersection with the output plane

Following reflection from the third sphere, the ray intersects the output plane. The ray reflected from the third sphere is described by the equation

$$\begin{aligned} \vec{r} &= \vec{r}_1(u_1, v_1) + \vec{s}_1(u_1, v_1)l_1 + \\ &+ \vec{s}_2(u_2, v_2)l_2 + \vec{s}_3(u_3, v_3)l_3. \end{aligned} \quad (25)$$

The intersection with the output plane is given by

$$\begin{aligned} \left(\vec{r}_1(u_1, v_1) + \vec{s}_1(u_1, v_1)l_1 + \right. \\ \left. + \vec{s}_2(u_2, v_2)l_2 + \vec{s}_3(u_3, v_3)l_3, \vec{m} \right) = 0. \end{aligned} \quad (26)$$

Solving Eq. (26) for l_3 , the point of intersection with the output plane is given by

$$\begin{aligned} \vec{r}_{out} &= \vec{r}_1(u_1, v_1) + \vec{s}_1(u_1, v_1)l_1 + \\ &+ \vec{s}_2(u_2, v_2)l_2 + \vec{s}_3(u_3, v_3)l_3. \end{aligned} \quad (27)$$

Considering that (u_2, v_2) and (u_3, v_3) depend on the coordinates of the point of ray intersection with the first sphere, the coordinates of the point of intersection with the output plane is a function of u_1, v_1 :

$$\vec{r}_{out} = \vec{r}_{out}(u_1, v_1). \quad (28)$$

Calculating the illuminance within a geometrical optics approach

In this section, we calculate the field from an optical element located on a curvilinear surface in a plane (\tilde{x}, \tilde{y}) found at distance \tilde{z} from the origin.

The energy conservation law is given by

$$I(u_1, v_1) \cdot |\vec{r}_u \times \vec{r}_v| \cdot \left(\vec{s}_0(u_1, v_1), \vec{n}(u_1, v_1) \right) du_1 dv_1 = \quad (29)$$

$$\int_{\vec{r}_{out}} I(x, y) dx dy \Big|_{\vec{r}_{out}} \Big|_{\perp}(u_1, v_1), \quad (30)$$

where l is the distance from the ray output point to the ray input point, and \vec{S}_2 is the direction of the outgoing ray from the surface.

$T(u_1, v_1)$ is the transmission coefficient for the ray that intersects the first sphere at point (u_1, v_1) . Then, making use of the property of the Dirac δ -function, the illuminance in the plane can be given by

$$\begin{aligned} I(r_{\perp}) &= \int \delta \left(r_{\perp} - \left(\vec{r}_{out} \right)_{\perp}(u_1, v_1) \right) I_0(u_1, v_1) \times \\ &\times T(u_1, v_1) \Big|_{\vec{r}_u \times \vec{r}_v} \Big|_{\perp} \left(\vec{S}_2(u_1, v_1) \cdot \vec{N} \right) du_1 dv_1. \end{aligned} \quad (31)$$

For practical purposes, when calculating Eq. (31) the Dirac δ -function is replaced with the approximate relation:

$$\delta(x, y) = a \exp \left(-\frac{x^2 + y^2}{\sigma^2} \right). \quad (32)$$

2. Asymptotic methods for calculating a coherent field from a DOE located on a curvilinear surface using the scalar theory

Let us analyze diffraction by a DOE located on a curvilinear surface and having a zone structure. Assume a diffractive microrelief coated on a curvilinear surface. Let the surface be described by the equations:

$$\begin{cases} x = x(u, v), \\ y = y(u, v), \\ z = z(u, v). \end{cases} \quad (33)$$

In the surface vicinity, we can introduce the curvilinear coordinates

$$x = X_2(u, v) = x(u, v) + N_x t, \quad (34)$$

$$y = Y_2(u, v) = y(u, v) + N_y t, \quad (35)$$

$$z = Z_2(u, v) = z(u, v) + N_z t. \quad (36)$$

Designate the permittivity in the surface vicinity as

$$\varepsilon(u, v, t) = \sum_n g_n(t) \exp(ikn\varphi(u, v)), k = \frac{2\pi}{\lambda}, \quad (37)$$

where λ is the wavelength. In a number of cases, the physical meaning of the function $\varphi(u, v)$ coincides with the eikonal function of the DOE.

Calculating a local DOE period on a curvilinear surface

Assume that the surface under study and the eikonal function on the surface are described by parametric relations:

$$\begin{cases} \bar{r} = \bar{r}(u, v), \\ \varphi = \varphi(u, v). \end{cases} \quad (38)$$

Let on the surface there be a curve described by the equation

$$\bar{r}(t) = \bar{r}(u(t), v(t)). \quad (39)$$

Let us find a surface direction along which the function remains unchanged. This direction can be derived from the condition given in the vector form:

$$\begin{cases} \frac{d\bar{r}}{dt} = \bar{r}_u(u, v) \frac{du}{dt} + \bar{r}_v(u, v) \frac{dv}{dt}, \\ \varphi_u(u, v) \frac{du}{dt} + \varphi_v(u, v) \frac{dv}{dt} = 0. \end{cases} \quad (40)$$

By expressing dv/dt from the second equation and substituting it into the first equation, we find the relation for the tangent vector along the curve

$$\bar{r}(t) = \bar{r}(u(t), v(t)), \quad (41)$$

$$\frac{d\bar{r}}{dt} = \left[(\varphi_v(u, v))^{-1} \frac{d\varphi}{dt} \right] \bar{B}_3, \quad (42)$$

$$\text{where } \bar{B}_3 = \varphi_v(u, v) \bar{r}_u(u, v) - \varphi_u(u, v) \bar{r}_v(u, v). \quad (43)$$

The direction of the vector \bar{B}_3 coincides with that of the tangent vector to the curve in question.

The unit vector \bar{b}_3 along this direction can be given by

$$\bar{b}_3(u, v) = \frac{\bar{B}_3(u, v)}{B_3(u, v)}. \quad (44)$$

Let us find the direction of the fastest change of the function. This direction is perpendicular to the vector \bar{b}_3 and to the normal vector \bar{N} to the surface:

$$\bar{b}_1 = \bar{b}_3 \times \bar{N},$$

$$\bar{B}_1(u, v) = [\bar{B}_3(u, v) \times \bar{N}(u, v)], \quad (45)$$

$$\bar{N}(u, v) = [\bar{r}_u(u, v) \times \bar{r}_v(u, v)].$$

Making use of the vector algebra relation

$$[a \times [b \times c]] = b(ac) - c(ab),$$

we obtain

$$\begin{aligned} \bar{B}_1(u, v) &= \left(\varphi_u(\bar{r}_v, \bar{r}_v) - \varphi_v(\bar{r}_u, \bar{r}_u) \right) \bar{r}_u + \\ &+ \left(\varphi_v(\bar{r}_u, \bar{r}_u) - \varphi_u(\bar{r}_v, \bar{r}_v) \right) \bar{r}_v. \end{aligned} \quad (46)$$

Now, we can determine how the increments du, dv are changing when the position of a surface point changes along the vector \bar{b}_1 by $d\bar{l}$:

$$\bar{r}_u(u, v) du + \bar{r}_v(u, v) dv = \frac{B_1}{B_1} d\bar{l}. \quad (47)$$

Performing sequential scalar multiplication of the vector equation by $\bar{r}_u(u, v), \bar{r}_v(u, v)$, we get a set of linear equations:

$$\begin{aligned} (\bar{r}_u(u, v) \bar{r}_u(u, v)) du + (\bar{r}_v(u, v) \bar{r}_u(u, v)) dv &= \\ = \frac{(B_1 \bar{r}_u(u, v))}{B_1} d\bar{l}, \end{aligned} \quad (48)$$

$$\begin{aligned} (\bar{r}_u(u, v) \bar{r}_v(u, v)) du + (\bar{r}_v(u, v) \bar{r}_v(u, v)) dv &= \\ = \frac{(B_1 \bar{r}_v(u, v))}{B_1} d\bar{l}. \end{aligned} \quad (49)$$

$$\text{where } (B_1 \bar{r}_u) = \varphi_u(u, v) D, \quad (50)$$

$$(B_1 \bar{r}_v) = \varphi_v(u, v) D, \quad (51)$$

$$\begin{aligned} D = N^2 &= (\bar{r}_u(u, v), \bar{r}_u(u, v)) (\bar{r}_v(u, v), \bar{r}_v(u, v)) - \\ &- (\bar{r}_v(u, v), \bar{r}_u(u, v))^2. \end{aligned} \quad (52)$$

Solving the set of linear equations gives

$$du = \left(\frac{\varphi_u(u, v) (\bar{r}_v(u, v), \bar{r}_v(u, v))}{B_1} - \right. \quad (53)$$

$$\left. - \frac{\varphi_v(u, v) (\bar{r}_u(u, v), \bar{r}_v(u, v))}{B_1} \right) d\bar{l},$$

$$dv = \left(\frac{\varphi_v(u, v) (\bar{r}_u(u, v), \bar{r}_u(u, v))}{B_1} - \right. \quad (54)$$

$$\left. - \frac{\varphi_u(u, v) (\bar{r}_v(u, v), \bar{r}_v(u, v))}{B_1} \right) d\bar{l}.$$

Substituting the relations for du, dv into the expression that describes the change of the function $\varphi(u, v)$ by 2π

$$\varphi_u(u, v) du + \varphi_v(u, v) dv = \frac{2\pi}{k}, \quad (55)$$

where k is the wavenumber, we obtain the relation for a local period of the diffraction grating:

$$d\bar{l} = \frac{2\pi N}{kB_3}. \quad (56)$$

Below, the local period is designated as d .

Calculating the direction of reflected and refracted rays upon diffraction by a DOE located on a curvilinear surface

Let us find a change in the direction of a ray refracted at a curvilinear surface coated with a diffractive microrelief. Assume that the surface is an interface between two media with refractive indices $\varepsilon_1, \varepsilon_2$. Let the ray be incident on the surface from the medium ε_1 . The ray direction is described by a vector \bar{S}_1 . The reflected rays are defined by the direction $\bar{S}_1^{(n)}$. The refracted

rays have the direction $\overline{S_2^{(n)}}$.

The directions of the refracted rays satisfy the following relations:

$$\begin{cases} \overline{S_2^{(n)}, \overline{b_1}} = (\overline{S_2}, \overline{b_1}) + (2\pi n) / (kd\sqrt{\varepsilon_2}), \\ \overline{S_2^{(n)}, \overline{b_3}} = (\overline{S_2}, \overline{b_3}), \\ (\overline{S_2^{(n)}, \overline{S_2^{(n)}}}) = 1. \end{cases} \quad (57)$$

The vector's directions $\overline{S_2} = \overline{S_2^{(0)}}$ are related with the incident ray vector $\overline{S_1}$ by the refraction law.

Directions of the reflected rays satisfy the relations:

$$\begin{cases} \overline{S_1^{(n)}, \overline{b_1}} = (\overline{S_1}, \overline{b_1}) + (2\pi n) / (kd\sqrt{\varepsilon_1}), \\ \overline{S_1^{(n)}, \overline{b_3}} = (\overline{S_1}, \overline{b_3}), \\ (\overline{S_1^{(n)}, \overline{S_1^{(n)}}}) = 1. \end{cases} \quad (58)$$

Here, n is the number of the ray. $\overline{S_1}$ is related with the incident ray direction by the reflection law. To be able to find the directions of the reflected and refracted rays at the medium interface where the DOE is located the incident ray direction needs to be known.

Let the eikonal $\varphi^0(u, v)$ in a medium with permittivity ε be defined on a surface described by parametric equations

$$\begin{cases} \overline{r} = \overline{r}(u, v), \\ \varphi = \varphi^0(u, v). \end{cases} \quad (59)$$

Let us derive the direction of rays generated by a wavefront with eikonal $\varphi^0(u, v)$. The direction of ray propagation can be found by solving the set of equations:

$$\begin{cases} (1/\sqrt{\varepsilon})\varphi_u^0(u, v) = (\overline{S}, \overline{r_u}) = S^x x_u + S^y y_u + S^z z_u, \\ (1/\sqrt{\varepsilon})\varphi_v^0(u, v) = (\overline{S}, \overline{r_v}) = S^x x_v + S^y y_v + S^z z_v, \\ (\overline{S}, \overline{S}) = 1. \end{cases} \quad (60)$$

The unit vector of the ray can be expanded in terms of tangent and normal vectors of the surface on which the eikonal of the incident field is defined:

$$\begin{cases} \overline{S} = p\overline{r_u} + q\overline{r_v} + t\overline{n}, \\ p = \frac{1}{D\sqrt{\varepsilon_2}} (\varphi_u^0(\overline{r_u}, \overline{r_v}) - \varphi_v^0(\overline{r_u}, \overline{r_v})) = \\ = \frac{1}{D\sqrt{\varepsilon_2}} (\varphi_u^0 r_v - \varphi_v^0 r_u) \overline{r_v}, \\ q = \frac{1}{D\sqrt{\varepsilon_2}} (-\varphi_u^0(\overline{r_u}, \overline{r_v}) + \varphi_v^0(\overline{r_u}, \overline{r_v})) = \\ = \frac{-1}{D\sqrt{\varepsilon_2}} (\varphi_u^0 r_v - \varphi_v^0 r_u) \overline{r_u}, \\ (\overline{S}, \overline{S}) = 1, \end{cases} \quad (61)$$

where

$$\begin{aligned} D(u, v) &= N^2 = \\ &= (\overline{r_u}(u, v), \overline{r_u}(u, v)) (\overline{r_v}(u, v), \overline{r_v}(u, v)) - \\ &\quad - (\overline{r_v}(u, v), \overline{r_u}(u, v))^2. \end{aligned} \quad (62)$$

It is seen from the relations above that the projection of the unit vector onto a tangent surface to the eikonal surface is given by

$$\overline{S}_\perp = \overline{B_1^0} / (D\sqrt{\varepsilon_2}), \quad (63)$$

$$\begin{aligned} \overline{B_1^0} &= (\varphi_u^0(\overline{r_u}, \overline{r_v}) - \varphi_v^0(\overline{r_u}, \overline{r_v})) \overline{r_u} + \\ &\quad + (\varphi_v^0(\overline{r_u}, \overline{r_u}) - \varphi_u^0(\overline{r_u}, \overline{r_v})) \overline{r_v}. \end{aligned} \quad (64)$$

The refraction law for the DOE takes the form:

$$\begin{aligned} \overline{S}_\perp^n &= \overline{S}_\perp + \frac{2\pi n}{kd\sqrt{\varepsilon_2}} \overline{b_1} = \\ &= \overline{S}_\perp + \frac{2\pi n \overline{B_1}}{kd\sqrt{\varepsilon_2} B_1} = \overline{S}_\perp + \frac{B_1}{\sqrt{\varepsilon_2} D}. \end{aligned} \quad (65)$$

Thus, we have derived an expression for the refracted ray at a diffractive element located on a curvilinear surface, which we will below employ to calculate the intensity within a geometrical optics approach.

Calculating the illuminance within a geometrical optics approach

In this section, we calculate the field in a plane (\tilde{x}, \tilde{y}) found at distance \tilde{z} from the optical element located on a curvilinear surface

$$\begin{aligned} I(u, v) \cdot [\overline{r_u} \times \overline{r_v}] \cdot (\overline{S_2}(u, v), \overline{N}(u, v)) du dv = \\ = I(\tilde{x}, \tilde{y}) d\tilde{x} d\tilde{y}, \end{aligned} \quad (66)$$

$$\begin{cases} \tilde{x} = x(u, v) + S_2^x \frac{(\tilde{z} - z(u, v))}{S_2^z}, \\ \tilde{y} = y(u, v) + S_2^y \frac{(\tilde{z} - z(u, v))}{S_2^z}, \end{cases} \quad (67)$$

where l is the distance from the ray output point to the input point, $\overline{S_2}$ is the unit vector of the outgoing ray.

The energy conservation law is

$$\begin{aligned} I(x, y) &= \int \delta(x - \tilde{x}(u, v), y - \tilde{y}(u, v)) \times \\ &\quad \times I_0(u, v) T(u, v) |\overline{r_u} \times \overline{r_v}| (\overline{S_2}(u, v), \overline{N}) du dv. \\ \begin{cases} \tilde{x} = x(u, v) + S_2^x \frac{(\tilde{z} - z(u, v))}{S_2^z}, \\ \tilde{y} = y(u, v) + S_2^y \frac{(\tilde{z} - z(u, v))}{S_2^z}, \end{cases} \end{aligned} \quad (68)$$

where ν is the transmission coefficient on the surface.

Calculating the local period of a DOE on a spherical surface

In this Section, we calculate the local period of a DOE located on a spherical surface. A particular case is presented by a diffraction grating on a spherical mirror, which is used in an Offner hyperspectrometer. The grating has no radial symmetry. Then, the parametric equation of the surface and the phase function of the grating are given by

$$\begin{cases} x = u, \\ y = v, \\ z = \sqrt{R_1^2 - u^2 - v^2}, \\ \varphi = \varphi(u). \end{cases} \quad (69)$$

It is worth noting that the parameters u, v represent the Cartesian coordinates on the sphere. The vectors $\vec{r}_u(u, v), \vec{r}_v(u, v)$ are given by

$$\begin{aligned} \vec{r}_u(u, v) &= \left(1, 0, -\frac{u}{z(u, v)} \right), \\ \vec{r}_v(u, v) &= \left(0, 1, -\frac{v}{z(u, v)} \right). \end{aligned} \quad (70)$$

The normal vector to a sphere of radius R for the surface defined by the above parametric equations takes the form:

$$\begin{aligned} \vec{N}(u, v) &= [\vec{r}_u(u, v) \times \vec{r}_v(u, v)] = \\ &= \left(\frac{u}{z(u, v)}, \frac{v}{z(u, v)}, 1 \right). \end{aligned}$$

We can write $\vec{b}_3 = \frac{B_3}{B_3}$, where \vec{B}_3 is given by

$$\vec{B}_3(u, v) = -\varphi_u(u, v)\vec{r}_u(u, v). \quad (71)$$

Let us find the direction of the function fastest growth. This direction is perpendicular to the vector \vec{b}_3 and to the normal vector \vec{N} to the surface.

$$\begin{aligned} \vec{b}_1(u, v) &= \frac{\vec{B}_1(u, v)}{B_1(u, v)}, \\ \vec{B}_1(u, v) &= [\vec{B}_3(u, v) \times \vec{N}(u, v)], \\ \vec{B}_1(u, v) &= \varphi_u(\vec{r}_u, \vec{r}_v)\vec{r}_u - \varphi_u(\vec{r}_u, \vec{r}_v)\vec{r}_v, \\ B_1(u, v) &= N(u, v)B_3(u, v), \\ \vec{B}_1(u, v) &= \varphi_u(\vec{r}_u, \vec{r}_v)\vec{r}_u - \varphi_u(\vec{r}_u, \vec{r}_v)\vec{r}_v. \end{aligned} \quad (72)$$

The local period is given by

$$d = \frac{2\pi N(u, v)}{kB_3(u, v)}. \quad (73)$$

The relations derived in the previous sections make it possible to calculate the direction of rays reflected from a convex mirror in the Offner scheme. The calculation procedures for ray tracing in the first and third mirrors remain unchanged. The relation to describe the intensity of the rays having arrived to a point also remains unchanged. An essential disadvantage of the proposed approach is that the intensity of a ray reflected from the diffraction grating cannot be calculated by means of geometrical optics. The reflection coefficient can be calculated only using the wave theory or, in some cases, even the vector electromagnetic theory [33].

Simulation of image acquisition in an Offner scheme with prisms using the Zemax software package

An Offner scheme with prisms depicted in Fig. 2 was described in Ref. [7]. In the left-hand side of the scheme there is a telescopic unit of focal length 300 mm, whereas the right-hand side unit contains dispersive elements in the form of two prisms P_1 and P_2 made of quartz glass. The right-hand side also has three spherical mirrors M_1, M_2 , and M_3 with respective radii -161.3 mm; -74.9 mm, and -153.5 mm. The image is registered in the plane of detector D.

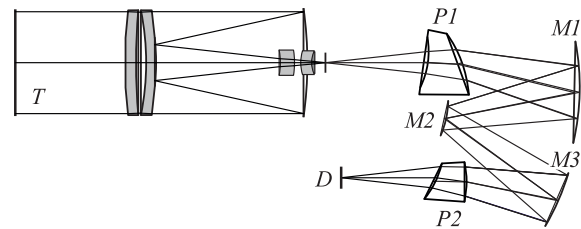


Fig. 2. Offner scheme with prisms.

The simulation results for the scheme of Fig. 2 presented in Figs. 3 and 4 have been derived using the Zemax software package [34].

The spread of spectral orders in a registration plane of diameter 16 mm for different wavelengths is shown in Fig. 3. The simulation was conducted for visible wavelengths (ranging from 0.4 μm to 1 μm) and IR wavelengths (ranging from 1.6 μm to 2.6 μm).

Patterns in Fig. 4 were acquired for the wavelengths presented in Fig. 3.

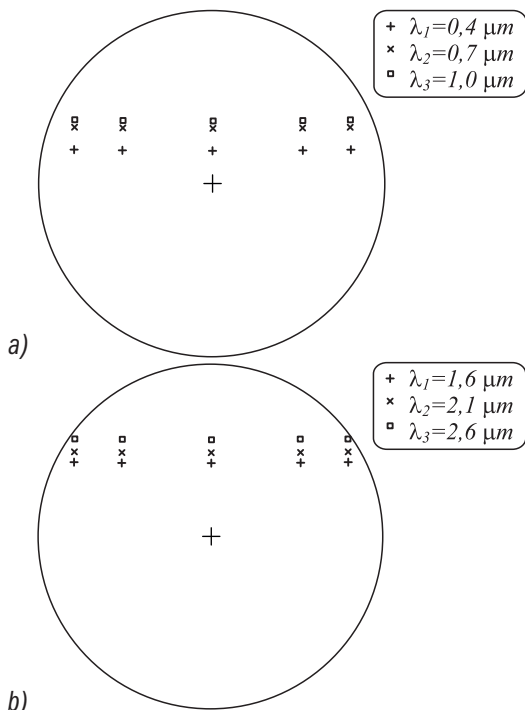


Fig. 3. Spread of spectral orders in the registration plane for different wavelengths λ_i : (a) visible range; (b) IR range.

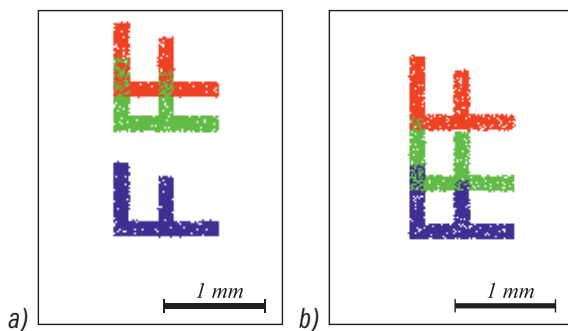


Fig. 4. Acquisition of a dispersed image of letter F: (a) visible wavelengths; (b) IR wavelengths.

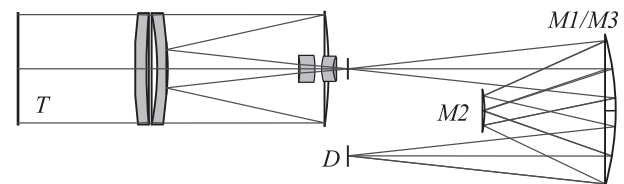


Fig. 5. Offner scheme with a diffraction grating.

The simulation results for such a scheme obtained using the Zemax software package are depicted in Figs. 6 and 7.

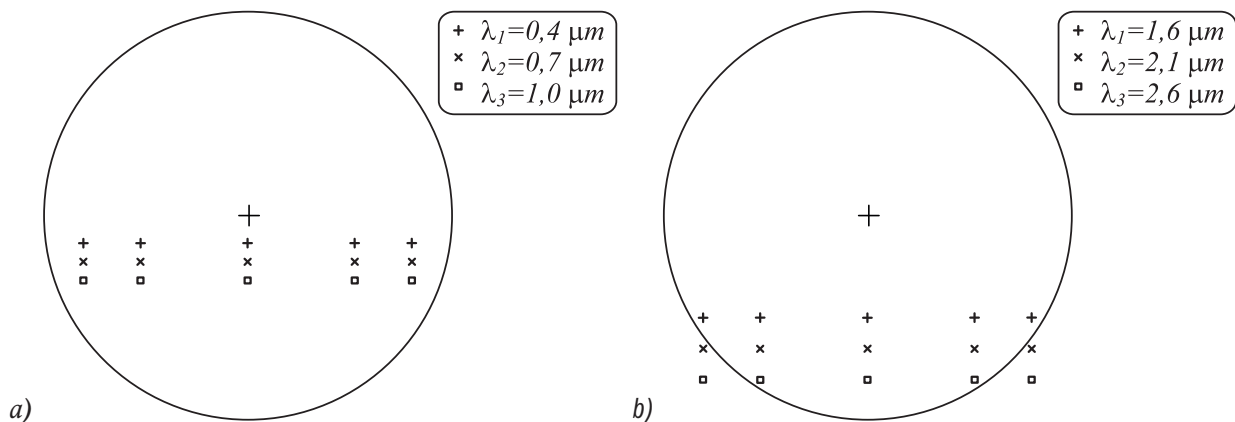


Fig. 6. Spread of the spectral orders in the registration plane for different wavelengths λ_i with a diffraction grating put in the scheme: (a) visible wavelength range; (b) IR wavelength range.

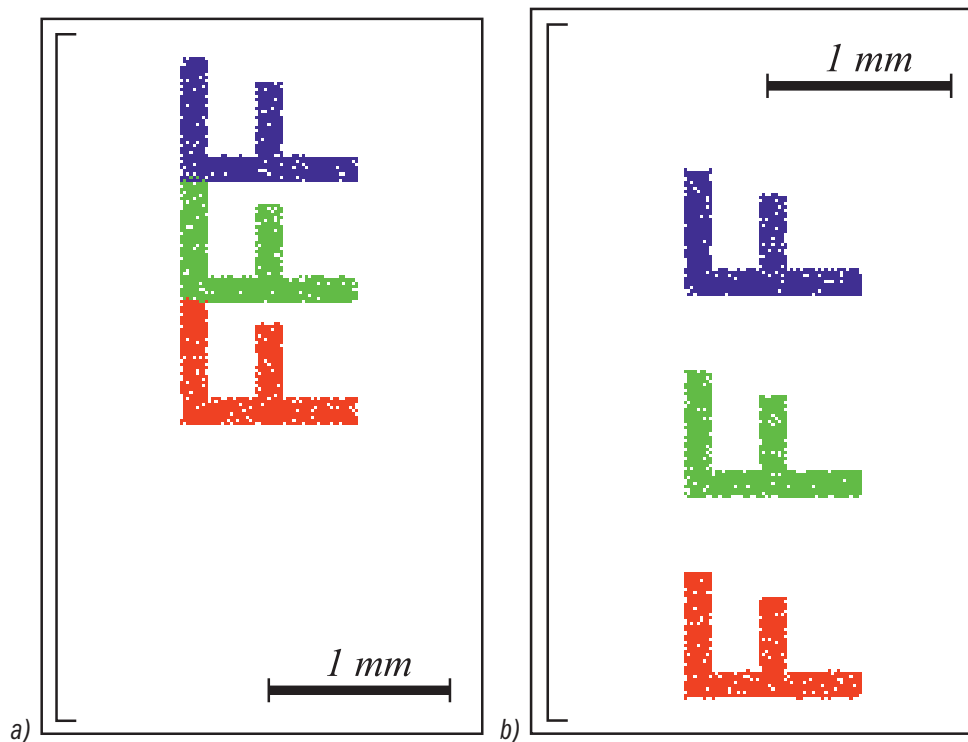


Fig. 7. Acquisition of a dispersed image of letter "F" when using a diffraction grating: (a) visible wavelengths; (b) IR wavelengths.

From the simulation results, the spread of spectral orders is seen to be uniform for different wavelength ranges. When compared with the prism-based schemes, this also offers an advantage (in addition to a lighter weight) as it simplifies image processing. It is worth noting that in the IR range the spread is larger. These factors contribute to the enhancement of spectral resolution.

Dispersed images of letter 'F' obtained at different wavelength ranges are shown in Fig. 7. The wavelengths used are the same as in Fig. 6. The spread for different wavelengths (visible and IR) is seen to have a linear dependence, with the spread for the IR range seen to be larger.

Conclusion

We have analyzed a geometrical-optical modeling of an imaging Offner hyperspectrometer based on prisms or a diffraction grating.

The use of the diffraction grating instead of prisms has been shown not only to lighten the overall weight of the optical system but also to result in a more uniform spread of dispersed image spectral components.

Acknowledgements

This work was partially funded by the RF Ministry of Education and Science and RFBR grants ## 13-07-12181 and 14-07-97008.

References

- I. Fursov, V.A.** Thematic classification of hyperspectral images based on conjugacy class / V.A. Fursov, S.A. Bibikov, O.A. Bajda // *Computer Optics*. – 2014. – Vol. 38(1). – P. 154-158. (In Russian).
- Zhuravel, Yu.N.** Specific features of hyperspectral remote sensing data processing in problems of environmental monitoring / Yu.N. Zhuravel, A.A. Fedoseev // *Computer Optics*. – 2013. – Vol. 37(4). – P. 471-476. (In Russian).
- Gashnikov, M.V.** Hierarchical grid interpolation for hyperspectral image compression / M.V. Gashnikov, N.I. Glumov // *Computer Optics*. – 2014. – Vol. 38(1). – P. 87-93. (In Russian).
- Green, R.O.** Imaging spectroscopy and the airborne visible/infrared imaging spectrometer (AVIRIS) / R.O. Green [et al.] // *Remote Sensing of Environment*. – 1998. – Vol. 65(3). – P. 227-248.
- Rickard, L.J.** HYDICE: An airborne system for hyperspectral imaging / L.J. Rickard [et al.] // *Opti-*

cal Engineering and Photonics in Aerospace Sensing. – 1993. – P. 173-179.

■ **6. Gelikonov, G.V.** A dispersive optical element for obtaining a linear optical spectrum / G.V. Gelikonov, V.M. Gelikonov, P.A. Shiljagin // Patent No. RU 2398193 C2. Date of Publication 27.08.2010 Bull. 24. (In Russian).

■ **7. Lee, J.H.** Optical Design of A Compact Imaging Spectrometer for STSAT3 / Jun Ho Lee, Tae Seong Jang, Ho-Soon Yang, Seung-Wu Rhee // Journal of the Optical Society of Korea. – 2008. – Vol. 12(4). – P. 262-268.

■ **8. Lee, J.H.** Optomechanical Design of a Compact Imaging Spectrometer for a Microsatellite STSAT3 / Jun Ho Lee, Chi Weon Lee, Yong Min Kim, Jae Wook Kim // Journal of the Optical Society of Korea. – 2009. – Vol. 13(2). – P. 193-200.

■ **9. Lee, J.H.** A very compact imaging spectrometer for the micro-satellite STSAT3 / Jun Ho Lee, Kyung In Kang, Jong Ho Park // International Journal of Remote Sensing. – 2011. – Vol. 32(14). – P. 3935-3946.

■ **10. Lee, J.H.** Flight Model Development of a Compact Imaging Spectrometer for a Microsatellite STSAT3 / Jun Ho Lee, Tae Seong Jang, Kyung In Kang, and Seung-Wu Rhee // Proc. of the conference "Optical Remote Sensing of the Environment", Tucson, AZ, June 7, 2010.

■ **11. Lobb, D.R.** Imaging spectrometer // Patent No. US 6288781 B1. Date of Publication 11.09.2001.

■ **12. Mouroulis, P.** Optical design of a compact imaging spectrometer for planetary mineralogy / P. Mouroulis, R.G. Sellar, D.W. Wilson // Optical Engineering. – 2007. – Vol. 46(6). – P. 063001-1-9.

■ **13. Mouroulis, P.** Convex grating types for concentric imaging spectrometers / P. Mouroulis, D.W. Wilson, P.D. Maker, R.E. Muller // Applied Optics. – 1998. – Vol. 37(31). – P. 7200-7208.

■ **14. Lobb, D.R.** Imaging spectrometer // Patent No. EP 0961920 B1. Date of Publication 12.05.2004.

■ **15. Chrisp, M.P.** Convex diffraction grating imaging spectrometer // Patent No. US 5880834 A. Date of Publication 9.03.1999.

■ **16. Reininger, F.M.** Imaging spectrometer/camera having convex grating // Patent No. US 6100974 A. Date of Publication 8.08.2000.

■ **17. Nelson, N.R.** Hyperspectral scene generator and method of use // Patent No. US 7106435 B2. Date of Publication 12.09.2006.

■ **18. Oskotsky, M.** Airborne hyperspectral imaging system // Patent No. US 7944559 B2 / M. Oskotsky, M.J. Russo, Jr. Date of Publication 17.05.2011.

■ **19. Offner, A.** An: 1.0 Camera for Astronomical Spectroscopy / A. Offner, W.B. Decker // Journal of the Optical Society of America. – 1951. – Vol. 41. – P. 169-169.

■ **20. Prieto-Blanco, X.** Off-plane anastigmatic imaging in Offner spectrometers / X. Prieto-Blanco, H. Gonzalez-Nuez, R. de la Fuente // Journal of the Optical Society of America A. – 2011. – Vol. 28. – P. 2332-2339.

■ **21. Gonzalez-Nuez, H.** Pupil aberrations in Offner spectrometers / H. Gonzalez-Nuez, X. Prieto-Blanco, R. de la Fuente // Journal of the Optical Society of America A. – 2012. – Vol. 29. – P. 442-449.

■ **22. Prieto-Blanco, X.** The Offner imaging spectrometer in quadrature / X. Prieto-Blanco, C. Montero-Orille, H. Gonzalez-Nuez, M.D. Mouriz, E.L. Lago, R. de la Fuente // Optics Express. – 2010. – Vol. 18. – P. 12756-12769.

■ **23. Prieto-Blanco, X.** Analytical design of an Offner imaging spectrometer / X. Prieto-Blanco, C. Montero-Orille, B. Couce, R. de la Fuente // Optics Express. – 2006. – Vol. 14. – P. 9156-9168.

■ **24. Johnson, W.R.** All-reflective snapshot hyperspectral imager for ultraviolet and infrared applications / W.R. Johnson, D.W. Wilson, G. Bearman // Optics Letters. – 2005. – Vol. 30. – P. 1464-1466.

■ **25. Labusov, V.A.** A multichannel spectrometer / V.A. Labusov, I.A. Zarubin, M.S. Saushkin // Patent No. RU 2375686 C2. Date of Publication 10.12.2009 Bull. 34.

■ **26. Tennant, W.E.** Graded order-sorting filter for hyperspectral imagers and methods of making the same // Patent No. US 7936528 B2. Date of Publication 3.05.2011.

■ **27. Norton, A.** Diffraction order sorting filter for optical metrology / A. Norton, H. Tuitje, F. Stanke // Patent No. US 8107073 B2. Date of Publication 31.01.2012.

■ **28. Buralli, D.A.** Optical performance of holographic kinoforms / D.A. Buralli, G.M. Morris, J.R. Rogers // Applied Optics. – 1989. – Vol. 28. – P. 976-983.

■ **29. Dammann, H.** Blazed synthetic phase only holograms / H. Dammann // Optik. – 1970. – Vol. 31. – P. 95-104.

■ **30. Mouroulis, P.** Optical design of a coastal ocean imaging spectrometer / P. Mouroulis, R.O. Green, D.W. Wilson // Optics Express. – 2008. – Vol. 16(12). – P. 9087-9096.

■ **31. Mouroulis, P.** Design of pushbroom imaging spectrometers for optimum recovery of spectroscopic and spatial information / P. Mouroulis, R.O. Green, T.G. Chrien // Applied Optics. – 2000. – Vol. 39(13). – P. 2210-2220.

■ **32. Kazanskiy, N.L.** Mathematical modeling of optical systems / N.L. Kazanskiy. – Samara: Samara State Aerospace University. – 2005. – P. 240.

33. *Diffractive Computers Optics* / D.L. Golovashkin, L.L. Doskolovich, N.L. Kazanskiy, V.V. Kotlyar, V.S. Pavelyev, R.V. Skidanov, V.A. Soifer, S.N. Khonina. – Ed. by V.A. Soifer. – Moscow: “Fizmatlit” Publishers. – 2007. – P. 736.
34. <http://www.zemax.com/> (Website) – Zemax software package. Description.

